

THE ACOUSTIC SHOWERGLASS. I. SEISMIC DIAGNOSTICS OF PHOTOSPHERIC MAGNETIC FIELDS

CHARLES LINDSEY AND D. C. BRAUN

Colorado Research Associates Division, NorthWest Research Associates, Inc., 3380 Mitchell Lane,
Boulder, CO 80301; clindsey@cora.nwra.com, dbraun@cora.nwra.com

Received 2004 February 5; accepted 2004 September 16

ABSTRACT

A problem of major interest in the helioseismology of active regions is the acoustics of magnetic photospheres and shallow subphotospheres. Magnetic fields suppress the photospheric signatures of acoustic waves impinging onto them from the underlying solar interior and shift their phases. The phase shifts function as a sort of acoustic showerglass that impairs the coherence of seismic waves arriving from below, degrading images of subsurface anomalies derived by mechanical reconstruction of phase-coherent waves. The purpose of this study is to characterize the “acoustic showerglass” in general optical terms and make a rough practical assessment of its impact on local seismic diagnostics of the shallow subphotospheres of active regions. We compile statistics comparing the acoustic field in magnetic photospheres with holographic projections of waves arriving from distant surrounding pupils. These “local control correlations” are consistent with an acoustic anomaly in the shallow subphotosphere of the active region that is strong but predominantly superficial; we call this the “acoustic Wilson depression.” The local control correlations also exhibit a phenomenon we call the “penumbral acoustic anomaly,” characterized by a conspicuous phase shift in regions of inclined magnetic field. This appears to be consistent with a fairly straightforward hydromechanical interpretation of the interaction of acoustic waves with photospheric magnetic forces. Detailed numerical simulations of the interaction of acoustic waves with magnetic forces can greatly facilitate our understanding of the acoustic showerglass and the thermal structure of the top few hundred kilometers of active region subphotospheres.

Subject headings: Sun: activity — Sun: helioseismology — sunspots

1. INTRODUCTION

1.1. *Seismology of Active Region Subphotospheres*

Over the past decade helioseismology has begun to focus on solar interior diagnostics from the local perspective, now recognized as local helioseismology. A major subject of interest to local helioseismology has been physical anomalies in the subphotospheres of active regions (e.g., Braun 1995; Duvall et al. 1996; Kosovichev et al. 2000). It is well established that active regions interact differently with active region photospheres than with the quiet photosphere. Active regions strongly absorb p -modes that reflect from them (Braun 1995). Computational holographic images of active regions show “acoustic moats” surrounding large sunspots (Lindsey & Braun 1998; Braun et al. 1998). Holographic imaging in the 5–6 mHz acoustic spectrum shows acoustic emission halos surrounding large, growing magnetic regions (Braun & Lindsey 1999; Donea et al. 2000). The basic mechanisms giving rise to these phenomena seem to be relatively superficial.

Hankel analysis and time-distance correlation measurements of waves reflected from active region photospheres consistently show travel times up to a minute less than for waves similarly reflected from the quiet photosphere (Braun 1995; Fan et al. 1995; Duvall et al. 1996; Hindman et al. 2000). Moreover, travel times for waves skipping from an active region photosphere to a distant point in the quiet photosphere are invariably less than for waves traveling along the same path but in the opposite direction (Duvall et al. 1996). Based on these travel time measurements, Duvall et al. (1996), Kosovichev (1996), and Kosovichev et al. (2000) propose models prescribing significant sound-speed anomalies (± 1 km s⁻¹) and rapid downflows (1–2 km s⁻¹) extending 10 Mm or more beneath sunspots. Numerical computations by Cally & Bogdan (1993),

Cally (2000), and Cally et al. (2003) simulating the interaction of acoustic waves with magnetic photospheres suggest that a considerable part of the phase perturbations that characterize active region photospheres could be accounted for by magnetic forces in the upper few hundred kilometers of the underlying subphotosphere. Because the superficial phase shifts by themselves can be quite large, they can significantly impair the coherence of acoustic waves arriving from the underlying active region subphotosphere. This imposes an effect similar to that of a showerglass in familiar electromagnetic optics.

The purpose of this study is to attempt a preliminary empirical assessment of the acoustics of active region magnetic fields and their function as an “acoustic showerglass.” We adapt techniques of computational seismic holography for this purpose, drawing from other familiar concepts in elementary optics. In this study we use correlations between the surface acoustic field in active regions and holographic projections of waves arriving there from the quiet Sun some distance away for an assessment of how active region photospheres respond to incoming acoustic waves differently from the quiet photosphere. We use the statistics of these correlations to develop a simple magnetic proxy for phase and amplitude perturbations that characterize the acoustic showerglass. The magnetic proxy can be used to correct showerglass perturbations for the purpose of imaging the underlying active region subphotosphere. This exercise will be the subject of a separate study (Lindsey & Braun 2005, hereafter Paper II).

1.2. *Basic Limitations of Acoustic Diagnostics*

In the context of local helioseismology, seismic holography can be regarded as computational seismology in the optical perspective. Optical diagnostics confront us with certain relatively rigid limitations. A major familiar example is diffraction, which

limits spatial discrimination of compact subphotospheric anomalies in the same way that electromagnetic diffraction limits the resolution of an optical microscope. Diffraction limits our horizontal discrimination of compact acoustic anomalies to separations of approximately a horizontal wavelength or more. It similarly limits our discrimination in depth. At first glance, diffraction may seem to be a serious disadvantage of optical diagnostics in particular. In fact, the liabilities of diffraction are quite general, and it is the optical perspective under which these are most clearly evident.

A second major difficulty that confronts local diagnostics of active regions in particular is the disproportionate acoustic signatures imposed by magnetic fields at the solar surface. A 1 kG magnetic field at the solar surface imposes a magnetic pressure perturbation, $B^2/(8\pi)$, comparable to the gas pressure at the base of the quiet photosphere, thereby exerting an effective sound-speed variation, $\Delta c/c$ of order unity. At a depth of 10 Mm the gas pressure is greater by a factor of 7×10^4 . This renders the fractional sound-speed variation of a 1 kG field, and the consequent phase perturbation, proportionately less.

Phase variations caused by thermal perturbations and flows a few megameters beneath the photosphere, while not nearly as small as those for magnetic fields, are nevertheless thought to be weak compared to equivalent perturbations at the surface (Lindsey et al. 1996). The practical imposition for active region diagnostics is the prospective function of strong surface magnetic fields to introduce phase uncertainties sufficient to obscure the signatures of local subphotospheric anomalies that might otherwise have been readily discernible.

1.3. The Acoustic Showerglass

The problem introduced by relatively large phase perturbations imposed at the solar surface has a clear analogy in the electromagnetic optics of commercial shower glass. The function of the showerglass is to confront the analyst who proposes to image electromagnetic radiation from behind it with phase uncertainties that render a coherent reconstruction of the source impractical even while the amplitude of the emergent radiation remains more than sufficient to detect the source. There are many familiar instances of clouds, fog banks, smoke screens, and other optical media passing sufficient radiation to illuminate the premises but destroying phase coherence so that stigmatic imaging of the source is rendered prohibitive. The particular distinction that the electromagnetic showerglass shares with active region photospheres is that it accomplishes this in a relatively thin surface. This greatly simplifies the problem of assessing and correcting the phase shifts, at least in principle.

The object of this study is to attempt a preliminary empirical assessment of the acoustic showerglass in terms of the dependence of the amplitude perturbation on certain aspects of the magnetic field. We try to assess the potential of vector magnetic maps as a proxy for the phase shifts. A tentative preliminary version of this study appears in Lindsey & Braun (2003). The study presented here represents a continuation and considerable expansion of certain aspects of the former one.

2. BASIC PRINCIPLES

2.1. Helioseismic Holography

The basic computational element of seismic holography is the partial extrapolation of the surface acoustic field into the solar interior, i.e., into the prospective neighborhoods of local acoustic anomalies. This is accomplished either forward or backward in time by computing fields of the form

$$H_{\pm}^{\mathcal{P}}(\mathbf{r}, \nu) = \int_{\mathcal{P}} d^2\mathbf{r}' G_{\pm}(|\mathbf{r} - \mathbf{r}'|, z, \nu) \psi(\mathbf{r}', \nu), \quad (1)$$

where $\psi(\mathbf{r}', \nu)$ represents the complex amplitude of the surface acoustic field at frequency ν and surface location \mathbf{r}' , and $G_{\pm}(|\mathbf{r} - \mathbf{r}'|, z, \nu)$ represents the Green's function that propagates an acoustic disturbance at a surface point, $\mathbf{R}' = (\mathbf{r}', 0)$, to a generally submerged "focal point," $\mathbf{R} = (\mathbf{r}, z)$, at depth z directly beneath surface point \mathbf{r} in an acoustic model devoid of anomalies. In these computations, \mathbf{r}' ranges over a surface region \mathcal{P} called the "pupil" of the computation (see Lindsey & Braun 2000). The focal point, $\mathbf{R} = (\mathbf{r}, z)$, of the computation most conveniently ranges over a submerged "focal plane" chosen by the analyst or a range of such planes covering depths of particular interest. The computation of the ingression, $H_{-}^{\mathcal{P}}$, at depth z from the surface acoustic field ψ can be regarded as a progression of the acoustic field forward in time from the surface into the solar interior. The egression, $H_{+}^{\mathcal{P}}$, is its time reverse, an acoustic regression. We represent these "holographic projections" by operators, $U_{-}^{\mathcal{P}}(z)$ and $U_{+}^{\mathcal{P}}(z)$, respectively, applied to the surface acoustic field ψ . Thus,

$$H_{\pm}^{\mathcal{P}}(z) = U_{\pm}^{\mathcal{P}}(z)\psi. \quad (2)$$

We sometimes use the term "progression" to indicate the generality, $U_{\pm}^{\mathcal{P}}$.

2.2. The Local Control Correlations

Standard phase-correlation holography of the subphotosphere generally compares maps of the correlation

$$C(\mathbf{r}, z) \equiv \langle H_{+}^{\mathcal{P}}(\mathbf{r}, z, \nu) H_{-}^{\mathcal{P}*}(\mathbf{r}, z, \nu) \rangle_{\Delta\nu} \quad (3)$$

between the acoustic egression and ingression at a common focal point, $\mathbf{R} = (\mathbf{r}, z)$, under a pupil configuration such as that shown in Figure 1a, illustrating what we call holography in the "lateral vantage." The angular brackets indicate an average over an appropriate positive range, $\Delta\nu$, in frequency. In this study we concentrate on diagnostics based on holography under the subjacent vantage, illustrated in Figure 1b, which makes it possible to image the surface from an extended surrounding pupil far from the focus. The surface focal point allows a direct comparison between the acoustic projections and the local acoustic field, ψ , at the focus. We can, for example, map the correlation

$$C_{\text{LC-}}(\mathbf{r}) \equiv \langle \psi(\mathbf{r}, \nu) H_{-}^{\mathcal{P}*}(\mathbf{r}, \nu) \rangle_{\Delta\nu} \quad (4)$$

between the ingression and the local acoustic amplitude at \mathbf{r} . If the pupil, \mathcal{P} , is predominantly a region on the quiet solar surface, and the focal point, $(\mathbf{r}, 0)$, is in a region of surface magnetic field \mathbf{B} , then the statistical relation between $C_{\text{LC-}}$ and \mathbf{B} should contain useful information on how surface magnetic fields shift the phase and amplitude of the local photospheric signatures of waves impinging into the neighborhood of $(\mathbf{r}, 0)$ from below.

A similarly useful diagnostic is derived from the correlation

$$C_{\text{LC+}}(\mathbf{r}) \equiv \langle H_{+}^{\mathcal{P}}(\mathbf{r}, \nu) \psi^*(\mathbf{r}, \nu) \rangle_{\Delta\nu} \quad (5)$$

between the local acoustic amplitude and the egression at \mathbf{r} . Just as the local acoustic amplitude contains the signature of waves impinging upward into the neighborhood of \mathbf{r} from \mathcal{P} , it

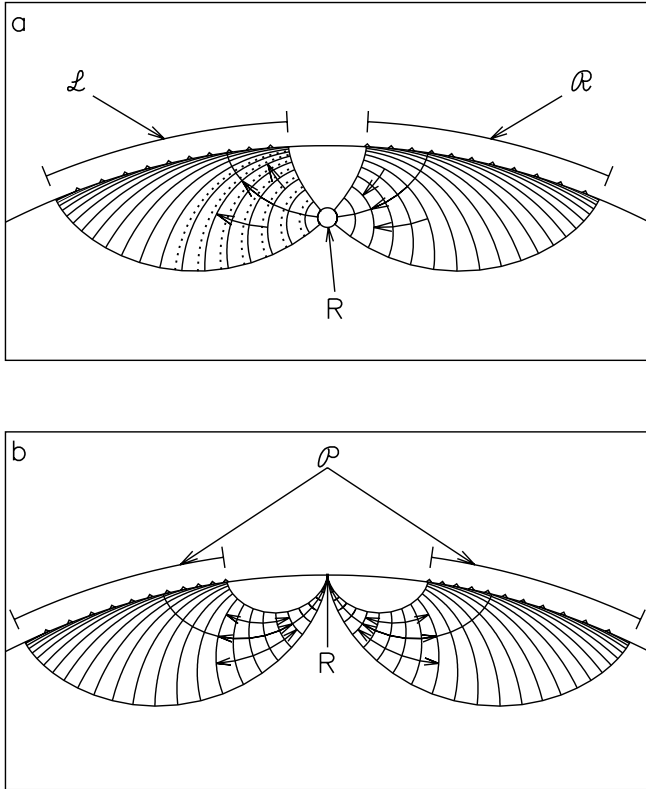


FIG. 1.—Conceptual diagrams illustrating (a) lateral-vantage seismic holography of a significantly submerged focal point, R , and (b) subjacent-vantage holography of a relatively shallow focal point, R , from an extended pupil, \mathcal{P} . The lateral vantage is used to reconstruct coherent phase-correlation images of submerged acoustic anomalies through the showerglass. The subjacent vantage, with R located at the solar surface, is used to compare the magnetic field, B , at R with the acoustic disturbance to and from \mathcal{P} , thereby assessing phase errors introduced as the acoustic disturbance passes through the underlying showerglass.

likewise contains the signature of downward-propagating waves, whether reflected from the surface or generated directly underneath in the neighborhood of r . These waves generally descend to some depth at which they are refracted back upward to reemerge at the surface minutes later, possibly in the pupil, \mathcal{P} . In the quiet Sun it is safe to assume that the relation between H_+^P and ψ is basically the time reverse of the relation between H_-^P and ψ . As a result, $C_{LC+} = C_{LC-}$ (Lindsey & Braun 2004). In § 3 we confirm that when r is in a magnetic region, C_{LC+} and C_{LC-} are significantly different in both modulus and phase. We call C_{LC-} and C_{LC+} the “local control correlations.” In particular, we refer to C_{LC-} as the “local ingression control correlation” and C_{LC+} as the “local egression control correlation.”

3. PROCEDURE

3.1. The Showerglass Measurements

In this section we map the local control correlations, $C_{LC\pm}$, in an active region and plot the statistical correlations between $C_{LC\pm}(r)$ and the strength, $B = |\mathbf{B}|$, of the magnetic field at r . We refer to these plots as “the showerglass measurements.” It is important to keep in mind that the showerglass measurements presented here are a rough initial assessment of the superficial anomaly immediately beneath r . Anomalies significantly beneath the photosphere will generally contribute something to the showerglass measurements. If these contributions are rel-

atively small, then the showerglass measurements will be relatively accurate. In the long run, discrimination between the showerglass and deeper underlying anomalies will be based on subsequent egression-ingression correlations over submerged focal planes. This will be the subject of a separate publication (Paper II).

Figures 2 and 3 show gray-scale maps of $C_{LC\pm}$ for NOAA AR 8179, normalized to real unity in the quiet Sun. These were computed from the Michelson Doppler Imager (MDI) line-of-sight velocity observations over a 24 hr period beginning at 11:00 UT on 1998 March 15. The observations were filtered for oscillations in the 4.5–5.5 mHz spectrum, and the acoustic projections, H_{\pm}^P , were computed over an annular pupil with an inner radius of 15 Mm and outer radius of 45 Mm. Figure 2 shows the individual real and imaginary parts of $C_{LC\pm}$.

The control correlations, $C_{LC\pm}$, can be conveniently represented in terms of their moduli, Γ_{\pm} , and phases, ϕ_{\pm} :

$$C_{LC\pm} = \Gamma_{\pm} \exp(i\phi_{\pm}), \quad (6)$$

where

$$\Gamma_{\pm} = |C_{LC\pm}|, \quad (7)$$

and

$$\phi_{\pm} = \arg C_{LC\pm}. \quad (8)$$

Figure 3 shows images of Γ_{\pm} and ϕ_{\pm} for AR 8179. The moduli, Γ_{\pm} , of the correlations are strongly suppressed in the magnetic regions, with the egression control correlation suppressed considerably more than the ingression. The local egression correlation phase signature, ϕ_+ , is conspicuously stronger than its ingression counterpart, ϕ_- . Note that the gray scale for ϕ_- is more sensitive than that for ϕ_+ by a factor of 2. The maximum signature in ϕ_- is approximately half that in ϕ_+ . Statistics of $C_{LC\pm}$ are plotted in Figures 4 and 5 as loci in the complex plane and as functions of the strength, B , of the surface magnetic field.

In these measurements, we did not take particular care to confine the pupil to regions of quiet Sun. As a result, the statistics plotted in Figures 4 and 5 could substantially overestimate ϕ_{\pm} . It should also be kept in mind that the phase shifts that appear in the statistics are due not only to the showerglass anomaly at the surface but to other anomalies through which the waves passed on their way to and from the focal point. On that account, the phases plotted in Figures 4 and 5 could further overestimate the phase shift introduced by the superficial anomaly alone. The moduli, $|C_{LC\pm}|$, of $C_{LC\pm}$ are plotted in Figure 6 along with the mean acoustic amplitude,

$$\psi_{\text{rms}} = \sqrt{\langle |\psi|^2 \rangle_{\Delta\omega}}, \quad (9)$$

which, like the correlations, is independently normalized to unity in the quiet Sun.¹ All three of these profiles are slightly

¹ Technically, what is plotted as ψ_{rms} in Fig. 6 is $[\langle |\psi(r, \nu)|^2 \rangle_{\Delta\omega}]^{1/2}$, whose units are consistent with those of $C_{LC\pm}$; however, it must be kept in mind that $\langle |\psi(\text{quiet Sun}, \nu)|^2 \rangle_{\Delta\omega}$ is unity in this presentation. The reason for this particular comparison is that the pupil for the H_{\pm}^P component of $C_{LC\pm}$ when r is in a sunspot umbra or strong magnetic region generally lies a considerable distance away, where the magnetic field is more typical of the quiet Sun. Consequently, only the ψ component of $C_{LC\pm}$ is substantially suppressed in the umbral photosphere. For the ideal case in which the umbra responded only to incoming acoustic waves with no additional noise, $C_{LC\pm}$ would be suppressed in the umbra in proportion to $|\psi|$.

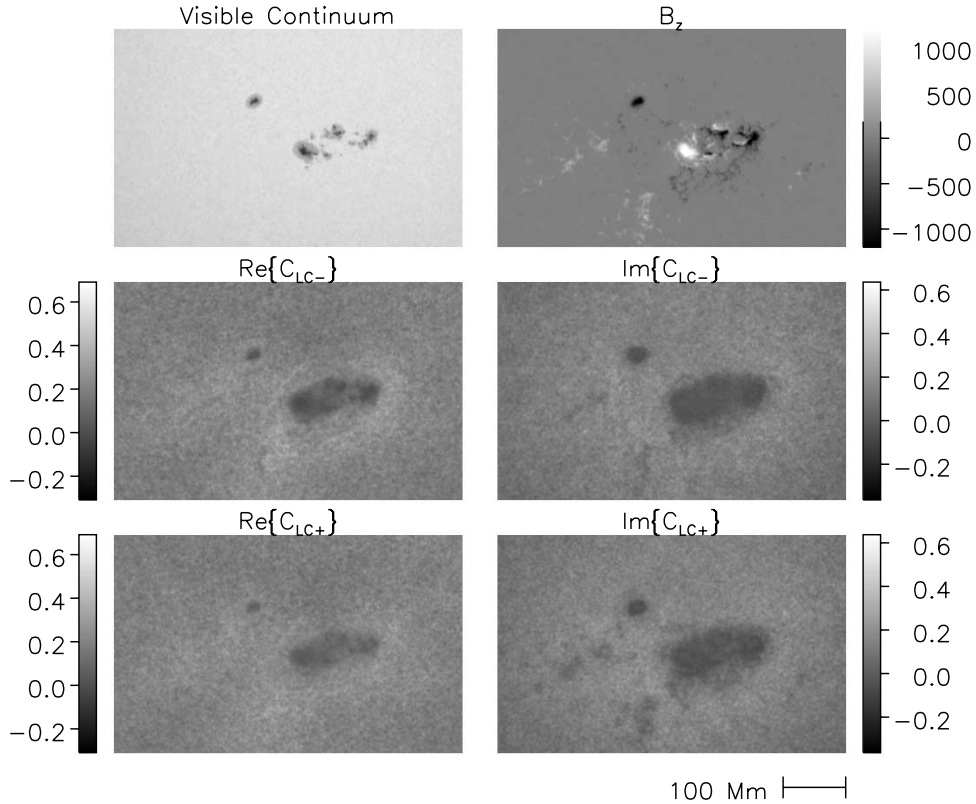


FIG. 2.—Gray-scale images of the local control correlations, C_{LC-} (middle row) and C_{LC+} (bottom row), compared with images of the visible continuum (top left) and vertical magnetic field, B_z (top right), for NOAA AR 8179. The local control correlations were integrated over a 24 hr period beginning at 11:00 UT on 1998 March 15. Visible continuum and line-of-sight magnetic images were recorded at 16:00 UT. The vector magnetic field, \mathbf{B} , was derived from a line-of-sight MDI magnetogram under the assumption that \mathbf{B} is the gradient of a potential. The top right frame shows the vertical component, B_z , of \mathbf{B} . In this figure $C_{LC\pm}$ is normalized to unity in the quiet Sun. The gray scales for the real and imaginary parts of $C_{LC\pm}$ are offset by ~ 0.32 times the quiet-Sun acoustic power to take advantage of the full available dynamic range of the color table.

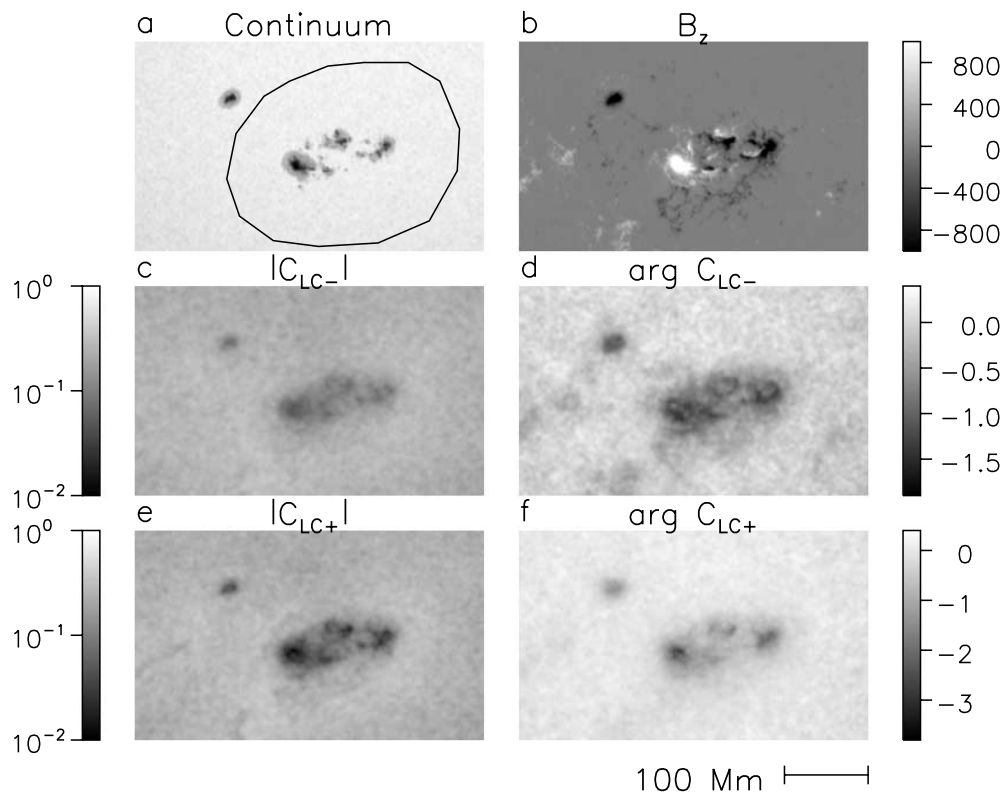


FIG. 3.—Gray-scale images of moduli (left column) and phase (right column) of the local control correlations, C_{LC-} (middle row) and C_{LC+} (bottom row), compared with images of the visible continuum (top left) and vertical magnetic field, B_z (top right), for NOAA AR 8179 (as in Fig. 2). The gray scales express moduli logarithmically, normalized to unity for the quiet Sun, and phase in radians. Note that the gray scale for ϕ_- is more sensitive than the gray scale for ϕ_+ by a factor of 2. The contour in the visible continuum map encloses the region over which the statistics of $C_{LC\pm}$ plotted in Figs. 4 and 5 were taken.

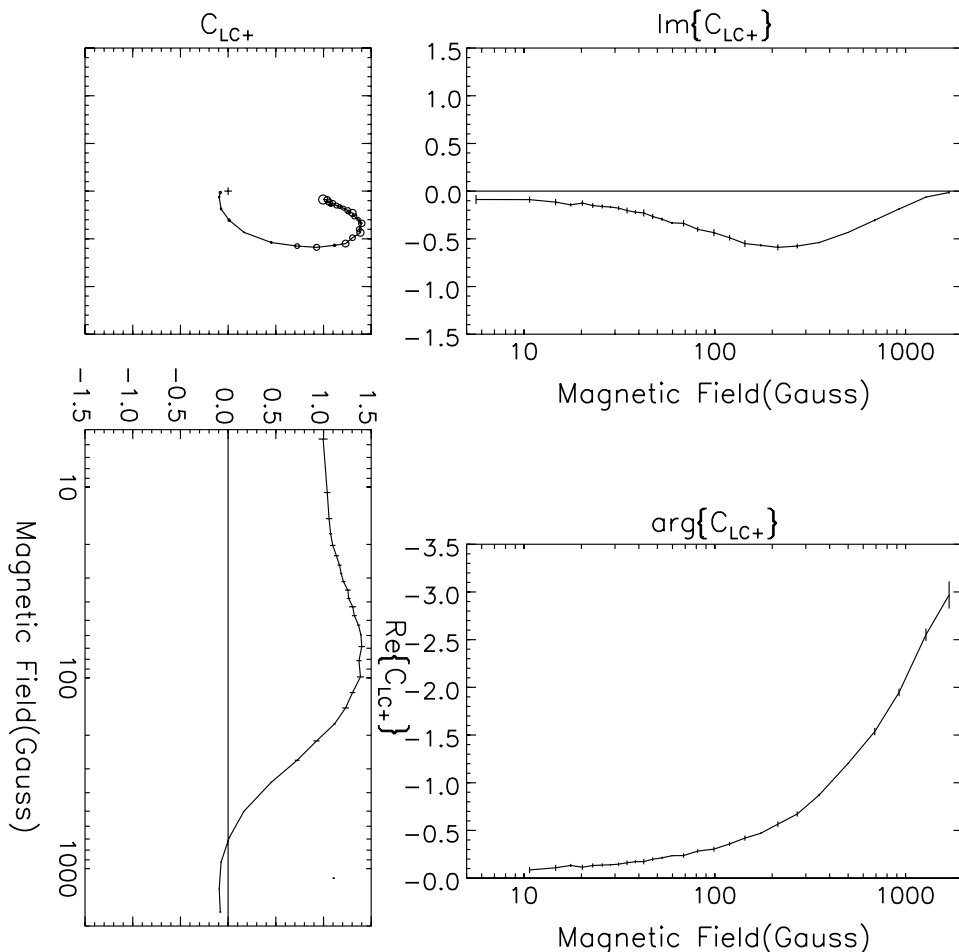


FIG. 4.—Diagnostic plots of the local egression control correlation, $C_{LC+} = \langle H_+^P \psi^* \rangle_{\Delta\nu}$, plotted as a function of the magnitude, B , of the magnetic field at the focal point over the region enclosing AR 8179 (indicated by the contour drawn in Fig. 3a). The control correlations were integrated over three consecutive 8 hr periods beginning on 1998 March 15 at 11:00 UT. The top left panel shows the locus of C_{LC+} in the complex plane over magnetic fields, B , ranging from 5 G to 2 kG. The bottom left panel shows the real part of C_{LC+} plotted as a function of B . The top right and lower right panels show the imaginary part of C_{LC+} and the argument of C_{LC+} (in radians), respectively, plotted as functions of B .

greater for B in the neighborhood of 100 G. Maximum values of 1.34, 1.46, and 1.10 are reached for $|C_{LC-}|$, $|C_{LC+}|$, and ψ_{rms} , respectively. For large B , all of the profiles decrease considerably. For B approaching 2 kG, ψ_{rms} is approximately half its value in the quiet Sun. The value of $|C_{LC-}|$ is less than ψ_{rms} by a factor of ~ 2.3 ; $|C_{LC+}|$, in turn, is less than $|C_{LC-}|$ by a factor of ~ 3 . The moduli plotted in Figure 6 are roughly consistent with a working interpretation that can be summarized in three points:

1. The Doppler sensitivity of the solar photosphere, as recorded by the MDI, to upcoming acoustic waves is considerably weaker in strong magnetic regions than that of the nonmagnetic photosphere. This explains why $|C_{LC-}|$ is substantially less in a magnetic photosphere than in the quiet Sun.
2. Only a fraction of the MDI Doppler signature of a strongly magnetic photosphere represents acoustic disturbances. This explains why $|C_{LC-}|$, normalized to the quiet Sun, is only a fraction of the same for ψ_{rms} in magnetic regions. We regard the non-acoustic component of ψ_{rms} as noise but note that the signal and noise together are less than the Doppler acoustic signature in the quiet Sun.
3. Strongly magnetic photospheres return only a fraction of the acoustic power that impinges into them from the solar interior. In the 2.5–4.5 mHz spectrum, this is attributed to strong ab-

sorption of upcoming acoustic waves in active regions, whereas the quiet Sun is an efficient reflector. In the 4.5–5.5 mHz spectrum, even the quiet Sun appears to absorb most of the upcoming wave flux, replacing it with newly generated acoustic radiation emitted downward. In this case, the deficit of downgoing wave flux from active regions suggests that less acoustic energy is locally generated in active regions. This explains why $|C_{LC+}|$ is only a fraction of $|C_{LC-}|$ in magnetic regions. The supposition behind this interpretation is that the solar surface registers downgoing waves, whether they are locally generated or reflections of upcoming waves, on terms similar to those for upcoming waves arriving from a considerable distance (Lindsey & Braun 2004). That the acoustic power emanating from strong magnetic regions is actually much less than that from the quiet Sun is supported by egression-power images (Lindsey & Braun 1998).

The phases, ϕ_{\pm} , of $C_{LC\pm}$ are plotted in Figure 7. The profiles of both ϕ_- and ϕ_+ show a consistently positive gradient with respect to $|B|$ for fields up to nearly 1 kG. The ranges of ϕ_- and ϕ_+ are equivalent to travel time reductions of up to 50 and 100 s, respectively, in strong magnetic regions.

The difference between ϕ_+ and ϕ_- is conspicuous in magnetic regions. This is the holographic representation in the 4.5–5.5 mHz band of the travel-time asymmetry discovered by

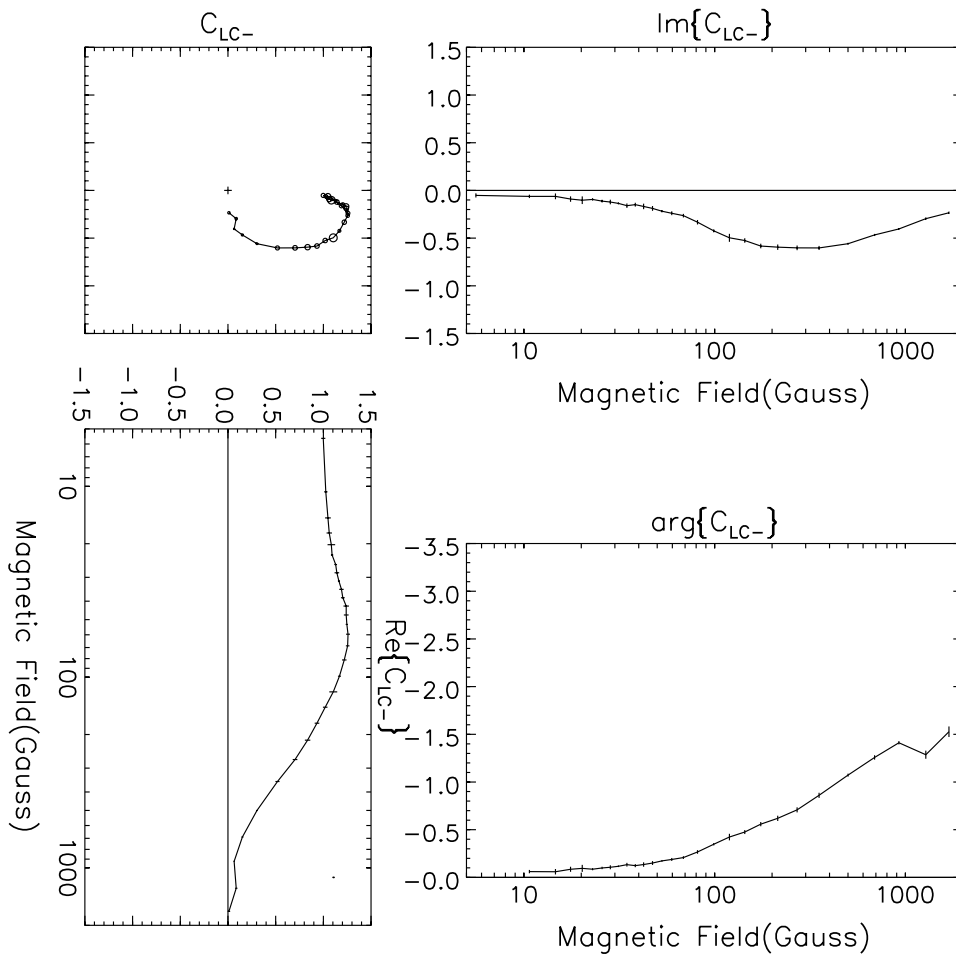


FIG. 5.—Diagnostic plots of the local ingestion control correlation, $C_{LC-} = \langle \psi H^{P*} \rangle_{\Delta\omega}$, plotted as for C_{LC+} in Fig. 4.

Duvall et al. (1996) from measurements of time-distance correlations over the ~ 2.5 – 4.5 mHz spectrum (see also Braun 1997). Figure 8 shows the phase asymmetry integrated over 1 mHz bands centered at 3, 4, and 5 mHz. In these maps the phases are rendered on a common gray scale for all frequen-

cies. In §§ 4.2 and 4.3 we develop the proposition that the phase asymmetry is the signature of a strong acoustic interaction with superficial magnetic fields. As such, it is regarded as characteristic of the acoustic showerglass.

At ~ 1 kG the profile of ϕ_- , plotted in Figure 7, undergoes a conspicuous inflection, while the gradient of ϕ_+ remains

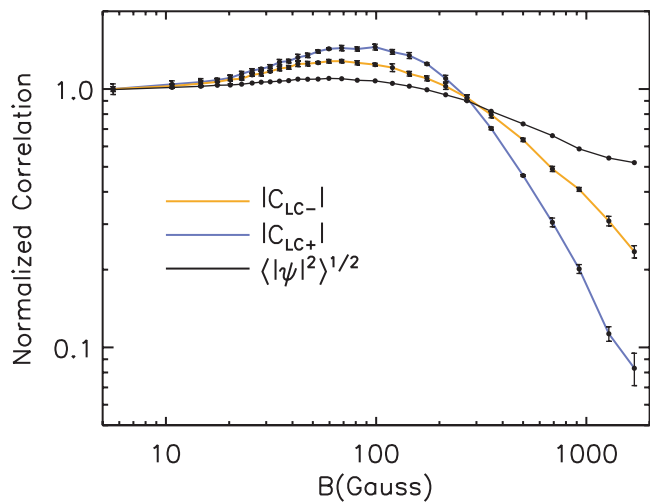


FIG. 6.—Moduli of the local control correlations, $|C_{LC-}|$ (yellow) and $|C_{LC+}|$ (blue), as functions of B taken from the diagnostic curves plotted in Figs. 4 and 5, plotted with the rms local acoustic amplitude, $\langle |\psi|^2 \rangle_{\Delta\nu}^{1/2}$ (black).

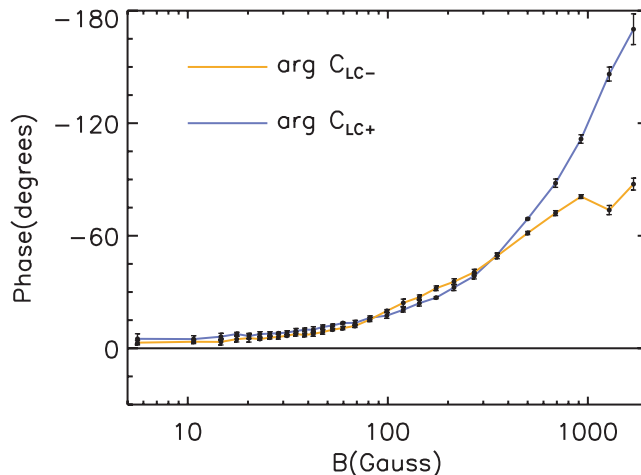


FIG. 7.—Plots of the arguments of C_{LC-} (yellow) and C_{LC+} (blue) from the diagnostic curves plotted in Figs. 4 and 5.

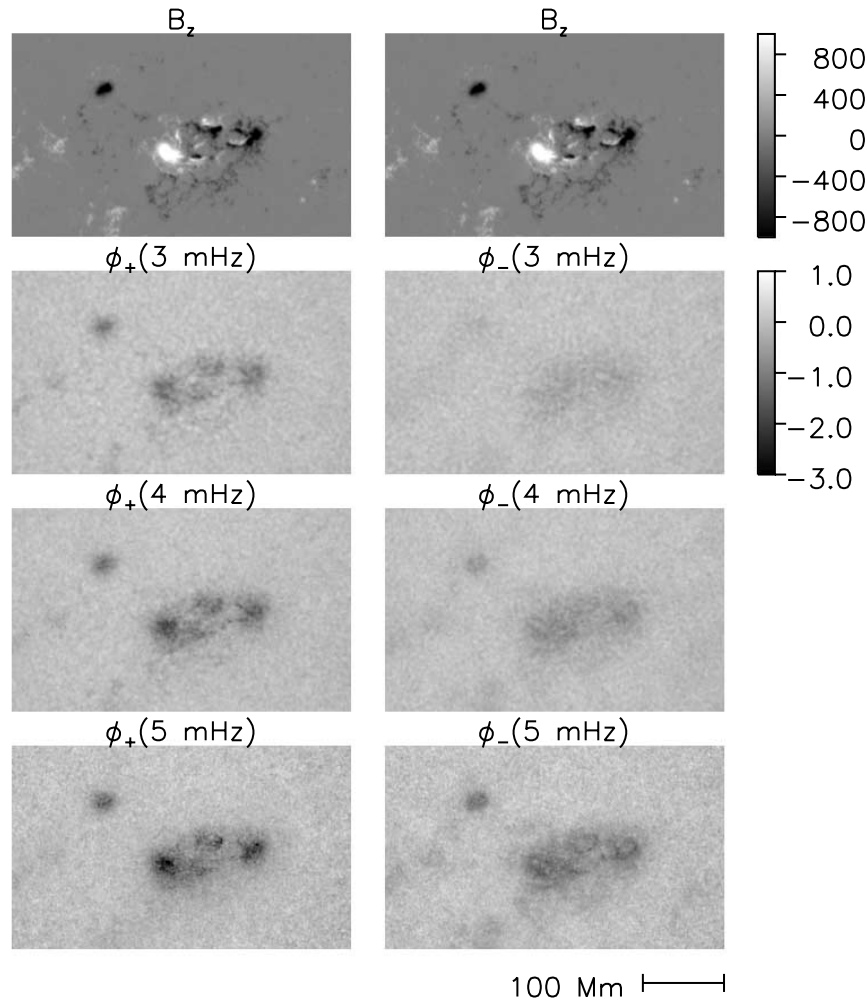


FIG. 8.—Maps of ϕ_+ (left column) and ϕ_- (right column) in AR 8179 integrated over 1 mHz bands centered at 3 mHz (second row), 4 mHz (third row), and 5 mHz (bottom row).

strongly positive. The somewhat erratic-looking reversal in the gradient of ϕ_- is the result of an effect that is quite significant and is clearly seen in the phase map of C_{LC-} rendered in Figure 3d. A careful examination of that image shows a systematic tendency for ϕ_- to reach a greater value well outside the sunspot umbra than anywhere in the umbra itself. This is a manifestation of a phenomenon that we call the “penumbral acoustic anomaly.” When the context is particularly the phase, ϕ_{\pm} , we usually use the more specific term “penumbral phase anomaly.” The penumbral phase anomaly appears to extend to lower frequencies (see Fig. 8), but the statistics are marginal in the 3 mHz spectrum due to diffraction.

The penumbral acoustic anomaly also appears in the relationship between the square magnetic field and the local acoustic power $|\psi|^2$, which, as we show in § 3.2, is excessively suppressed in the penumbrae and near outskirts of sunspots. We discuss the physical significance of the penumbral acoustic anomaly at length in § 4.3.

3.2. A Magnetic Proxy for the Showerglass

Adaptive optics offers a considerable range of techniques for correcting stochastic phase perturbations introduced by impositions such as turbulence in the terrestrial atmosphere. For helioseismic applications, the advent of Stokes magnetography from the Helioseismic Magnetic Imager (HMI) on the *Solar*

Dynamics Observatory (SDO) offers the prospect of a powerful magnetic proxy to correct showerglass phase perturbations. The liability of a magnetic proxy is the possibility of systematic errors. For example, the thermal structures of the top megameter of an umbral subphotosphere may evolve with time, introducing phase shifts for which the magnetic field by itself cannot account. The overwhelming advantage of the proxy, if the acoustics of the magnetic field are realistically assessed, would be statistical. Vector magnetic snapshots from the HMI will have far greater signal-to-noise than acoustic observations integrated over many hours. In any case, there are strong reasons to anticipate that a proxy will be useful in some capacity—for diagnostics of the upper megameters of the active region subphotosphere, if not for layers that lie a considerable distance beneath. In the exercise that follows, we fashion an exploratory proxy in which showerglass phase errors are approximated as a simple function of B^2 . We apply this proxy in a separate publication (Paper II) to image the subphotospheres of active regions to a depth of 10 Mm.

Braun (1997) proposed that the phase inequality between ϕ_+ and ϕ_- (see Fig. 7) is at least in considerable part a relatively superficial phenomenon, originating within a few megameters beneath the photosphere, and that it is significant over a broad range of frequencies for moderate or greater magnetic fields. On that basis we proceed here to treat the phase asymmetry

as part of the acoustic showerglass. Based on the considerable difference between ϕ_+ and ϕ_- in general, it is natural to fashion a proxy that applies a different phase correction to the local acoustic amplitude, ψ , for an egression computation than for an ingression computation. The general formalism for the correction is to multiply ψ by appropriate complex correction factors,

$$\psi_{\pm} = \Lambda_{\pm} \psi, \quad (10)$$

before applying the acoustic progressions, $U_{\pm}^P(z)$, to ψ_{\pm} :

$$H_{\pm}^P(z) = U_{\pm}^P(z) \psi_{\pm}. \quad (11)$$

In the absence of noise, the correction proxy for egression computations would be straightforward:²

$$\Lambda_+ = \frac{1}{C_{LC-}} = \frac{1}{\Gamma_-} \exp(-i\phi_-). \quad (12)$$

The appropriate proxy for ingression computations would be slightly more subtle:³

$$\Lambda_- = \frac{1}{\Gamma_-} \exp(-i\phi_+). \quad (13)$$

Figure 9 shows acoustic power maps of MDI Doppler observations with various modulus corrections applied. Figure 9a shows a map of the vertical magnetic field, B_z , reconstructed from an MDI line-of-sight magnetogram of AR 8179 under the potential field assumption. The magnetogram was taken on 1998 March 15 at 16:00 UT. Figure 9b shows the acoustic power map of the uncorrected Doppler observations integrated over the 4.5–5.5 mHz spectrum and the 24 hr period beginning on 1998 March 15 at 11:00 UT. Figure 9c shows the acoustic power map for Doppler observations corrected by the proxy described in the previous paragraph. The proxy-corrected acoustic power explodes in sunspot umbrae and penumbrae, since $|C_{LC-}|$ is only a fraction of ψ_{rms} . To avert the ill effects of umbral explosions, we retreat to a relative compromise,

$$\Lambda_{\pm} = \frac{1}{\psi_{\text{rms}}} \exp(-i\phi_{\mp}), \quad (14)$$

which limits the damage done by noise at the cost of under-representing the acoustic suppression that characterizes strong

² The logic in using ϕ_- to correct H_+^P is probably best illustrated with an example. The ingression in C_{LC-} represents waves that, in the showerglass measurements, traveled downward from the pupil, \mathcal{P} , and back upward to arrive at the surface focal point, r , located in some magnetic region. If we now want to compute the egression at some *submerged* focal point for which the pupil \mathcal{P} contains a magnetic region, the radiation of interest is traveling upward into the pupil, just as it was when it arrived at the magnetic focal point, r , during our measurement of C_{LC-} . It is therefore C_{LC-} that tells us what the magnetic region did to the phase of the acoustic radiation we propose to regress back into the solar interior. A similar argument in time reverse applies to the proxy for the ingression.

³ We adhere to $1/\Gamma_-$ to correct the modulus even while we switch to ϕ_+ for the phase. We are convinced that the reason Γ_+ is less than Γ_- is that the amplitude of the acoustic radiation leaving the magnetic region for the focal point is truly reduced. To apply $1/\Gamma_+$ would therefore be misrepresenting the reduced acoustic radiation that actually arrives at the focal point. The choice of $1/\Gamma_-$ assumes that the magnetic photosphere suppresses the surface signature of radiation leaving the pupil by the same factor as that of radiation arriving from a distant source.

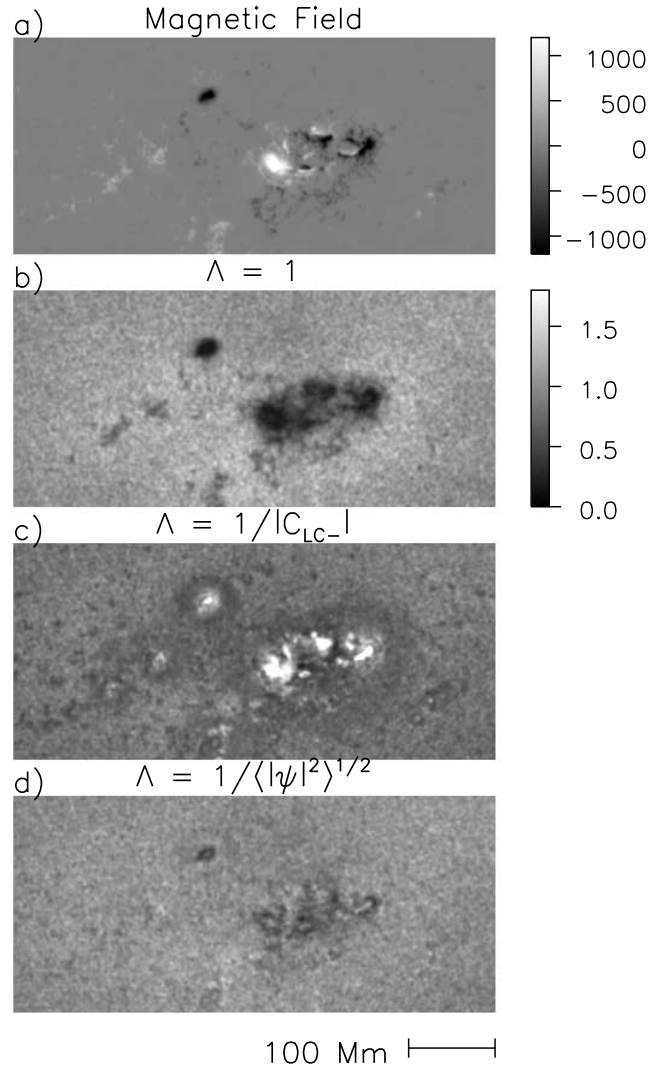


FIG. 9.—Acoustic power maps of the local acoustic amplitude, ψ , with various prospective corrections for the ingression showerglass. (a) Vertical magnetic field at 16:00 UT. (b) Acoustic power in the 4.5–5.5 mHz band integrated over the 24 hr period beginning at 11:00 UT. (c) Same as (b) but with ψ corrected for the showerglass as proposed by eq. (11). (d) Same as (b) but with ψ corrected for the showerglass as proposed by eq. (13).

magnetic regions. Figure 9d shows an acoustic power map of the same MDI Doppler observations as above corrected by the compromise proxy. The acoustic power variations seen in this map are considerably smaller but still substantial. In this case, the corrected acoustic power map shows conspicuous rings of relatively depressed acoustic power marking sunspot penumbrae and their relatively near outskirts. These ringlike depressions represent a second encounter with the penumbral acoustic anomaly introduced in § 3.1.

4. DISCUSSION

4.1. The Acoustic Wilson Depression

The phase signatures of the local control correlation, $\arg C_{LC\pm}$, are invariably negative (see Fig. 3, *light gray*) in magnetic regions with respect to the quiet Sun, indicating reduced one-way travel times both to and from the magnetic photosphere. The local ingression control correlation is consistent with a magnetic photosphere that is depressed several hundred km. More particularly, the approximately 90° phase shift shown by the

ingression control correlation for sunspot umbrae corresponds to a travel time deficit of 50 s. This could be modeled by removing the top 450 km of the active region photosphere. While such a model can apparently be made to work moderately well acoustically, it does not appear to be realistic to accomplish such a depression with magnetic forces consistent with observed photospheric fields. The magnetic pressure, $B^2/(8\pi)$, for a field of 2000 G is 1.6×10^5 dyne cm^{-2} , compared with a gas pressure of 6.0×10^5 dyne cm^{-2} 450 km beneath the photosphere (Christensen-Dalsgaard et al. 1993).

While it is probably safe to accept that a substantial physical depression of the magnetic photosphere by magnetic forces is a significant contributor to the phases that characterize the local control correlations, it is evident that the reality is considerably more complicated. A significant part of the signature could be the result of a significantly increased sound speed in the 0–5 Mm magnetic subphotosphere (Fan et al. 1995).

In this study we generalize the term “acoustic Wilson depression” to include any superficial mechanism, or anomaly based thereon, that contributes a phase shift that characterizes the local control correlations, whether or not it is based on a literal physical depression of the photosphere. It should therefore be understood in this study, as in Lindsey & Braun (2004), that we are now using this term in a more general sense than in earlier work (e.g., Braun & Lindsey 2000). The choice of this formalism is based on the simplicity and convenience of modeling a considerable range of superficial acoustic anomalies in terms of physical depressions and the ability of such models to fit the helioseismic correlations remarkably well in certain respects. However, we now turn our attention to some qualities of the active region acoustic signature that cannot be explained by a photospheric depression alone.

4.2. The Phase Asymmetry

The local control correlations, $C_{LC\pm}$, are the signature of some very interesting physics in the acoustics of magnetic subphotospheres that we are only now beginning to understand. One of the more conspicuous anomalies that characterizes $C_{LC\pm}$ is the considerably greater value of the local egression control phase, ϕ_+ , in strong magnetic fields than that of the ingression control phase, ϕ_- . This “phase asymmetry” was discovered by Duvall et al. (1996). They proposed an interpretation in terms of rapid downflows beneath sunspots that was developed at length by Kosovichev (1996). Braun (1997) cites several alternative factors characterizing dynamics of the relatively shallow subphotosphere that could give rise to the phase asymmetry. The phase asymmetry must be the signature of some process that is irreversible with respect to temporal progression in the interaction between acoustic waves and the local photospheric and subphotospheric anomalies that represent magnetic regions. For example, in the 4.5–5.5 mHz spectrum the phase asymmetry could be the result of a moderate depression of the characteristic depth, z_S (see Fig. 7b of Lindsey & Braun 2004 and related discussion in text), at which acoustic waves are generated in the magnetic subphotosphere. The physical mechanism that accounts for strong absorption of the p -modes could likewise be a major contributor to the phase asymmetry in the 2.5–4.5 mHz spectrum. In this context, the phase asymmetry may be largely a character of the interaction between acoustic fields and magnetic forces in the photosphere and shallow subphotosphere. This prospect leads to an examination of the penumbral acoustic anomaly introduced in § 3.1.

4.3. The Penumbral Acoustic Anomaly

Where considerations of discrimination with respect to time reversal are concerned, it is the *phase* of the penumbral acoustic anomaly, i.e., the “penumbral phase anomaly,” that is of particular interest. The penumbral phase anomaly characterizes a strong tendency for the phase, ϕ_- , of the local ingression control correlation, C_{LC-} , to reach a disproportionately large value in the sunspot penumbrae and their near outskirts, frequently reaching a maximum well outside the sunspot umbra and relaxing to a significantly lesser value in the umbra itself.

To begin with, it is helpful to recognize, in the 4.5–5.5 mHz spectrum in which the quiet photosphere is a significant absorber, that the interpretation of ϕ_- in terms of acoustics in a magnetic region is simpler than that of ϕ_+ in certain respects. When the pupil is in the quiet Sun, the local ingression control correlation, C_{LC-} , simply characterizes how the local magnetic photosphere acoustically responds to upcoming waves focused into it from a distant source, in this case the outlying annular pupil. By comparison, the local egression correlation, C_{LC+} , involves, in addition to the response of the local magnetic photosphere to upcoming waves, questions of how downgoing waves are generated differently in the magnetic subphotosphere than in the quiet Sun and the phase relation between the downgoing waves and the upgoing waves that register at the directly overlying photosphere. For example, C_{LC+} is critically dependent on how waves are generated differently in the active region subphotosphere than in the nonmagnetic subphotosphere, particularly where the distribution in depth is concerned. Its counterpart, C_{LC-} , can be regarded as securely independent of these concerns. It characterizes only how the magnetic photosphere responds to waves arriving from the quiet pupil, as prescribed by the ingression, H_-^P .

The penumbral phase anomaly, characterizing ϕ_- , imposes that the penumbrae and near outskirts of sunspots advance the phase of upcoming acoustic radiation disproportionately, even while the umbral photosphere is thought to have a greater magnetic field and Wilson depression. The reduced phase advance in the sunspot umbra suggests a region of reduced sound speed extending to a substantial depth beneath the umbral photosphere. Models by Kosovichev et al. (2000) propose sound-speed reductions in the range $0.5\text{--}1$ km s^{-1} from 0 to 3 Mm beneath sunspot umbrae with a horizontal extent comparable to or somewhat less than that of the umbra.

Based on increasingly compelling work by Cally & Bogdan (1993), Cally (2000), and Cally et al. (2003), we propose a substantially alternative interpretation of the penumbral phase anomaly based on the physics of the direct interaction between magnetic fields and acoustic waves. Cally (2000) argues that the interaction between acoustic waves and surface magnetic fields is generally strongly dependent on the inclination of the magnetic field with respect to the direction of propagation. At least in principle, a surface magnetic field, \mathbf{B} , scatters and absorbs a vertically propagating wave much more strongly if \mathbf{B} is substantially inclined with respect to the vertical direction than if it is vertical. The arguments of Cally (2000) are supported by detailed numerical modeling and reinforced by more recent analysis by Cally et al. (2003).

The spectrum of upcoming acoustic waves represented by the pupil of the showerglass measurements, an annulus with an inner radius of 15 Mm, is encompassed by a cone of inclination up to about 20° from vertical. In showerglass measurements made with pupils that have a larger inner radius representing

a narrower cone, the penumbral phase anomaly persists and, indeed, strengthens, although the statistics are poorer in proportion to the coarser spatial resolution as a result of diffraction and the reduced phase space encompassed by the narrower cone.

Based on Cally (2000), we currently believe that the substantially inclined magnetic fields that generally characterize the penumbrae and near outskirts of active regions are a major, if not the predominant, contributor to the penumbral phase anomaly. A rough intuitive concept of the function of inclined magnetic fields in this capacity can be derived by considering the simple comparative case of an electrical transmission line representing the subphotosphere terminated by various electrical components representing the solar surface. We represent the quiet solar surface by terminating the transmission with an electrical short. The introduction of a magnetic modulus at the solar surface can be represented by replacing the electrical short with a capacitor. The capacitor advances the phase of the current at the terminal by 90° with respect to that of a line terminated by an electrical short, for example. The inclined magnetic field also couples the predominantly vertical motion of the wave with a slow-mode Alfvén mode, in which the motion is predominantly horizontal and into which a substantial fraction of the incident energy flux absconds. This is the mechanism by which Cally (2000) proposes that compressional waves are substantially absorbed. The Alfvén mode can then be represented by a characteristic impedance that functions as a damper, reducing but not generally eliminating the phase shift introduced by the magnetic modulus. The electrical analogy is the introduction of a resistor in series with the terminating capacitor.

The actual dynamics of the interaction between acoustic waves and magnetic fields in three dimensions are considerably more complicated than the analogy to an electrical transmission line. We do not propose to resolve this problem in this study. It should, however, be recognized that a clear understanding of the direct interaction between surface magnetic fields and acoustic waves is a critical requirement for discrimination of the Doppler and thermal structure of the upper megameter of the subphotospheres of magnetic regions, and it is probably no less critical for that of the 1–10 Mm layer directly beneath.

4.4. The Quality of the MDI Doppler Observations

Notwithstanding the difficulties presented by the severe suppression of $|C_{LC+}|$ in sunspot umbrae, we note that $|C_{LC-}|$ in strong magnetic fields, including the sunspot umbra, while considerably less than in the quiet Sun, is quite significant with respect to the suppressed acoustic amplitude (see Fig. 6). The modulus of the local ingress control correlation, $|C_{LC-}| = |\langle \psi H_-^{P*} \rangle_{\Delta\omega}|$, measures the response of the sunspot umbra to waves focused into it (from the 15–45 Mm surrounding pupil). The plot of $|C_{LC-}|$ in Figure 6 establishes that approximately 20% of the umbral Doppler signal power represents the local acoustic disturbance in terms of acoustic power.⁴ This suggests that the MDI is getting a more substantial measurement of the actual acoustic field in large sunspot umbrae than the helioseismic community may be aware of.

The 80% of the signal power that remains can be regarded as noise for acoustic purposes. Whether this is instrumental noise or motion of the sunspot umbra that is independent of

acoustic disturbances is not clear to us. Cleaner observations of the umbral acoustic signal would be useful. This might be readily accomplished by extending helioseismic observations of sunspots into the near-IR spectrum, 1.5–2.5 μm , in which the relative brightness of sunspot umbrae with respect to the quiet Sun is considerably greater than in the visible spectrum and contamination by scattered light can be greatly reduced. If instrumental noise is important, its substantial reduction or elimination would improve acoustic diagnostics of umbral subphotospheres considerably.

The small value of $|C_{LC+}|$ relative to $|C_{LC-}|$ in the 4.5–5.5 mHz spectrum (see Fig. 6) is almost certain to be mostly the result of considerably suppressed acoustic emission downward into the solar interior from magnetic subphotospheres. (A similar relative suppression of $|C_{LC+}|$ in the 2.5–4.5 mHz spectrum is attributable to strong p -mode absorption of those frequencies by magnetic regions in which the quiet photosphere is an efficient reflector. In either case, the downward propagating flux in the magnetic region is generally much less than the upward propagating flux from the outlying quiet subphotosphere.) While the elimination of instrumental noise cannot be expected to substantially improve the imbalance between $|C_{LC+}|$ and $|C_{LC-}|$ in sunspot umbrae, it would nevertheless clearly improve the statistics of both $|C_{LC-}|$ and $|C_{LC+}|$ individually.

5. SUMMARY

Correlation statistics between holographic projections and local acoustic fields in active regions in the 4.5–5.5 mHz spectrum show signatures suggesting a strong, superficial acoustic anomaly directly beneath active regions. It is evident that the shallow magnetic subphotosphere can introduce phase shifts up to 90° into acoustic waves impinging into the photosphere from the underlying solar interior. These phase shifts can significantly impair the coherence of acoustic emission from submerged sources or scatterers, degrading phase-correlation statistics and images of subphotospheric anomalies computed by phase-coherent acoustic reconstruction. Because of this, we refer to this anomaly as the “acoustic showerglass.”

We characterize the acoustic showerglass in terms of the “local control correlations,” $C_{LC+} = \langle H_+^P \psi^* \rangle$ and $C_{LC-} = \langle \psi H_-^{P*} \rangle$, between subjacent acoustic progressions, H_\pm^P , to a surface focal point, r , from a distant pupil, and the local acoustic field, ψ , at r . The local control correlations show travel time deficits up to 50 s for C_{LC-} and 100 s for C_{LC+} . To model a 50 s travel time deficit in terms of a photospheric depression and no other anomalies would require the removal of the upper ~ 450 km of the magnetic photosphere. While a physical depression of the magnetic photosphere is probably a significant contributor to the local control correlation signatures, these signatures are evidently also indicative of other aspects of the interaction of acoustic waves with magnetic fields and perhaps a significant thermal enhancement in the upper megameter of the umbral subphotosphere. The large inequality in phase between C_{LC-} and C_{LC+} may be related to aspects of the acoustics of magnetic fields that result in significant absorption of p -modes in magnetic regions.

Comparisons between the local ingress control correlation, C_{LC-} , and the local square magnetic field, B^2 , reveal a conspicuous phase enhancement on the outskirts of sunspots, which we call the “penumbral acoustic anomaly.” The outskirts of sunspots are also characterized by a significant relative suppression in acoustic amplitude. We propose that the penumbral acoustic anomaly is largely a result of substantially

⁴ In terms of amplitude, the ratio is $\sim 45\%$.

inclined magnetic fields in the penumbrae and near outskirts of sunspots.

In our opinion, what is now most particularly needed in practical terms for realistic thermal models of active region subphotospheres is:

1. A more discriminating magnetic proxy that takes account of the inclination of the magnetic field.
2. The extension of the magnetic proxy to include frequencies from 2.5 to 4.5 mHz and possibly frequencies above 5.5 mHz.
3. Applications of the proxy to correct the surface acoustic field for holographic images of the underlying subphotosphere.

The third item in the list above is the subject of Paper II. A realistic magnetic proxy representing the acoustics of photospheric magnetic fields would have broad applications to active region seismology at large, not just to holographic computations. The first and second items in the list would benefit from the facility to run detailed hydromechanical computations of acoustic noise propagating through user-specified local acoustic anomalies over the spectrum encompassing known solar interior acoustics. Simulated sound computations, properly formulated and applied to realistic models of prospective acoustic anomalies, including a detailed account of photospheric and shallow subphotospheric magnetic forces with realistically inclined mag-

netic fields and magnetically depressed photospheres, would provide a powerful diagnostic tool for control purposes accessible to any helioseismic diagnostic technique that can be applied to actual helioseismic observations. In our opinion, credible simulated sound computations have become the crux of a clear understanding of the subphotospheres of active regions. We now regard this as a fundamental requirement for control work in the local helioseismology of active region subphotospheres.

We dedicate the work reported in this paper to the memory of Karen Harvey (1942–2002). C. Lindsey worked under the sponsorship of the Solar Physics Research Corporation for a significant part of the period of this research. We greatly appreciate consultation with P. S. Cally and H. Schunker at Monash University regarding their work on the acoustics of shallow subphotospheric magnetic fields. We also appreciate a large number of corrections and other very thoughtful suggestions and comments by the anonymous referee. This research was supported by grants from the Stellar Astronomy and Astrophysics Program of the National Science Foundation and the Sun-Earth Connection/Living With a Star and Supporting Research and Technology programs of the National Aeronautics and Space Administration.

REFERENCES

- Braun, D. C. 1995, *ApJ*, 451, 859
 ———. 1997, *ApJ*, 487, 447
 Braun, D. C., & Lindsey, C. 1999, *ApJ*, 513, L79
 ———. 2000, *Sol. Phys.*, 192, 307
 Braun, D. C., Lindsey, C., Fan, Y., & Fagan, M. 1998, *ApJ*, 502, 968
 Cally, P. S. 2000, *Sol. Phys.*, 192, 395
 Cally, P. S., & Bogdan, T. L. 1993, *ApJ*, 402, 721
 Cally, P. S., Crouch, A. D., & Braun, D. C. 2003, *MNRAS*, 346, 381
 Christensen-Dalsgaard, J., Proffitt, C. R., & Thompson, M. J. 1993, *ApJ*, 403, L75
 Donea, A.-C., Lindsey, C., & Braun, D. C. 2000, *Sol. Phys.*, 192, 321
 Duvall, T. L., Jr., D'Silva, S., Jefferies, S. M., Harvey, J. W., & Schou, J. 1996, *Nature*, 379, 235
 Fan, Y., Braun, D. C., & Chou, D.-Y. 1995, *ApJ*, 451, 877
 Hindman, B. W., Haber, D. A., Toomre, J., & Bogart, R. 2000, *Sol. Phys.*, 192, 363
 Kosovichev, A. G. 1996, *ApJ*, 461, L55
 Kosovichev, A. G., Duvall, T. L., Jr., & Scherrer, P. H. 2000, *Sol. Phys.*, 192, 159
 Lindsey, C., & Braun, D. C. 1998, *ApJ*, 499, L99
 ———. 2000, *Sol. Phys.*, 192, 261
 ———. 2003, in *Proc. SOHO 12/GONG+ 2002* (ESA SP-517; Noordwijk: ESA), 23
 ———. 2004, *ApJS*, 155, 209
 ———. 2005, *ApJ*, 620, 1118 (Paper II)
 Lindsey, C., Braun, D. C., Jefferies, S. M., Woodard, M. F., Fan, Y., Gu, Y., & Redfield, S. 1996, *ApJ*, 470, 636